

Cite this: *J. Mater. Chem. A*, 2019, 7, 11331

Swelling of graphene oxide membranes in alcohols: effects of molecule size and air ageing†

Artem Iakunkov,^a Jinhua Sun,^a Anastasia Rebrikova,^b Mikhail Korobov,^b Alexey Klechikov,^{ac} Alexei Vorobiev,^c Nicolas Boulanger^a and Alexandr V. Talyzin^{id}*^a

Swelling of Hummers graphene oxide (HGO) membranes in a set of progressively longer liquid alcohols (methanol to 1-nonanol) was studied using synchrotron radiation XRD after air ageing over prolonged periods of time. Both precursor graphite oxides and freshly prepared HGO membranes were found to swell in the whole set of nine liquid alcohols with an increase of interlayer spacing from ~ 7 Å (solvent free) up to ~ 26 Å (in 1-nonanol). A pronounced effect of ageing on swelling in alcohols was found for HGO membranes stored in air. The HGO membranes aged for 0.5–1.5 years show progressively slower swelling kinetics, a non-monotonic decrease of saturated swelling in some alcohols and complete disappearance of swelling for alcohol molecules larger than hexanol. Moreover, the HGO membranes stored under ambient conditions for 5 years showed a nearly complete absence of swelling in all alcohols but preserved swelling in water. In contrast, precursor graphite oxide powder showed unmodified swelling in alcohols even after 4 years of ageing. Since the swelling defines the size of permeation channels, the ageing effect is one of the important parameters which could explain the strong variation in reported filtration/separation properties of GO membranes. The time and conditions of air storage require standardization for better reproducibility of results related to performance of GO membranes in various applications. The ageing of GO membranes can be considered not only as a hindrance/degradation for certain applications, but also as a method to tune the swelling properties of HGO membranes for better selectivity in sorption of solvents and for achieving better selective permeability.

Received 19th February 2019
Accepted 2nd April 2019

DOI: 10.1039/c9ta01902b

rsc.li/materials-a

Introduction

Multilayered graphene oxide (GO) laminates in the form of papers,¹ thin films² or membranes^{3–5} have attracted a lot of attention over the past 6 years. The membranes have been proposed for various applications *e.g.* gas separation,⁶ nano-filtration,^{7–9} separation of solvent mixtures,^{10,11} as a toxicant barrier¹² and for water desalination.¹³

Graphite oxides are hydrophilic layered materials which can easily be dispersed in polar solvents.^{7,14} Drop casting⁵ and spin coating¹⁵ are the methods commonly used for preparation of GO thin films while vacuum filtration provides free standing membranes.^{16,17} Most of the applications cited above are enabled by the ability of GO multilayers to swell in polar solvents similarly to their precursor graphite oxides.^{18–20}

Swelling of GO membranes is directly related to the size of “permeation channels” which enable diffusion of solvents and

solutions. The interlayer distance of GO structures is typically studied using X-ray diffraction (XRD),^{14,21,22} direct measurement of film/membrane thickness²³ or quantitative evaluation of solvent vapor sorption.^{24–26} Simultaneous evaluation of multilayered GO film thickness and amount of sorbed solvent can be performed using Neutron Reflectivity (NR) methods.^{15,27}

Swelling of precursor graphite oxides in polar solvents has been studied in detail over the past 150 years, most typically in water,^{21,28} alcohols^{29–32} or amines.^{33–35} The swelling of graphite oxides depends on the synthesis method, most notably for materials prepared by Brodie's and Hummers' oxidation routes.³⁶ It is known that the interlayer distance of Brodie graphite oxides immersed in liquid alcohols increases proportionally to the length of molecules providing multilayered intercalation³⁰ with interlayer distances up to ~ 50 Å for 18-carbon molecules.²⁹

However, recent studies have revealed that the swelling of GO membranes can be significantly different compared to that of precursor graphite oxides.^{16,17} The swelling of GO membranes in *e.g.* liquid ethanol was reported with significant variation providing $d(001)$ values in the range ~ 11 – 17.7 Å.^{10,16,37,38} Swelling of HGO membranes was also reported once in several other alcohols: 1-propanol, 1-butanol and 1-pentanol.¹⁰ There have been no systematic studies available so far on swelling of

^aDepartment of Physics, Umeå University, S-90187, Umeå, Sweden. E-mail: alexandr.talyzin@umu.se

^bDepartment of Chemistry, Moscow State University, Leninskie Gory 1-3, Moscow 119991, Russia

^cDepartment of Physics and Astronomy, Uppsala University, Uppsala, 751 20, Sweden

† Electronic supplementary information (ESI) available. See DOI: 10.1039/c9ta01902b



either Hummers graphite oxides or GO membranes in larger alcohols.

Large variations can also be found in the literature for many other properties of GO membranes, including two orders of magnitude difference in permeation rates.³⁹ Recent studies emphasized the strong need for standardization of parameters affecting the performance of GO membranes, *e.g.* difference in oxidation degree, size and shape of GO flakes, defects, *etc.*^{39,40}

Little attention has so far been paid to the effects of GO membrane ageing.^{41,42} Metastability of the GO structure was reported for thin films but only over short periods of time (100 days) and mostly using X-ray Photoelectron Spectroscopy (XPS) which provides information about 1–2 surface layers of materials.⁴³ To our knowledge, the ageing of GO membranes during air storage has never been studied using characterization of bulk material properties.

Here we studied GO membranes prepared in 2012–2017 (ref. 16) and freshly prepared samples for swelling in a set of nine alcohols (from methanol to 1-nonanol). Prolonged storage of GO membranes in air is found to result in progressively slower kinetics of swelling, non-monotonic decrease of saturated swelling in some alcohols, and complete absence of swelling in alcohols after a certain period of ageing. At the same time no ageing effect was found for swelling of precursor graphite oxide powders even after 4 years of air storage. Therefore, the time and conditions of air storage need be considered for better reproducibility of GO membrane research.

Results and discussion

The GO membranes were studied by our group starting from 2012,^{16,17,24,44} including characterization of swelling in liquid water, ethanol and water–ethanol mixtures.¹⁶ The remaining pieces of the same membrane samples were stored in air for up to five years and tested again to verify for possible ageing effects.

Remarkably, the 5 year old sample showed a nearly complete absence of swelling in ethanol and larger alcohols (Fig. 1). The $d(001)$ of the HGO1 membrane back in 2012 was found to be 7.7 Å in the solvent free state and in liquid water, respectively. The $d(001)$ of the 5 year old HGO1 membrane was found to be nearly unchanged (7.8 Å) but immersion in ethanol resulted in lattice expansion only up to 8.1 Å. However, immersing the old sample into water provided a $d(001)$ value of 10.6 Å (12.3 Å back in 2012), thus demonstrating smaller but still significant swelling. Very similar results were also observed for the HGO1 thin film studied for swelling in saturated deuterated d_6 -ethanol vapour using the NR method three times with intervals of two years (see the ESI file†). The sorption of d_6 -ethanol decreased from 0.30 mol per formula unit (f.u.) to 0.07 mol perf.u. after four years of air storage and the d -spacing calculated from the change of the film thickness decreased from 10.0 Å to 8.6 Å. Note that the $d(001)$ observed for this film under ambient air conditions remained almost unchanged (8.1 Å and 8.3 Å for the pristine and 4 year old film). Moreover, we observed that films prepared using a freshly prepared aqueous GO dispersion and using the same dispersion after two years of storage showed no difference in swelling properties.

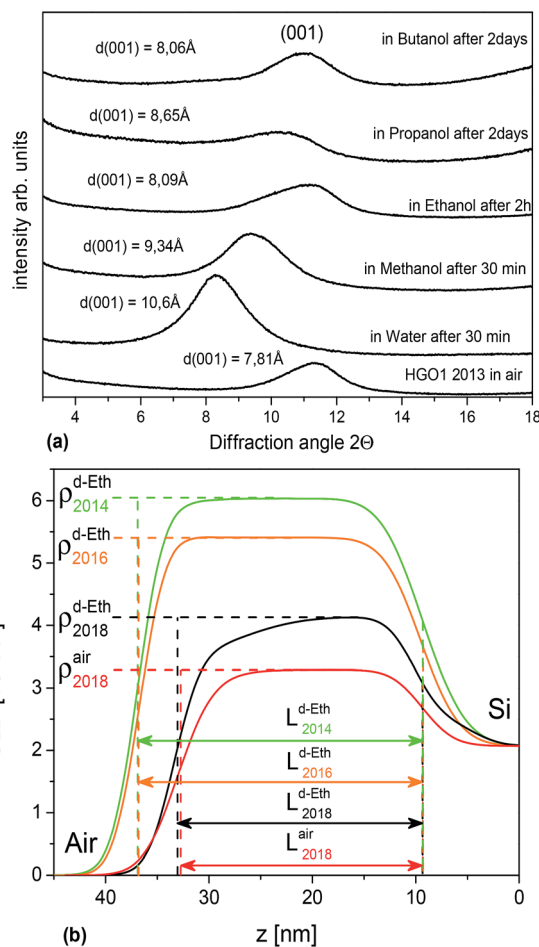


Fig. 1 (a) Saturated swelling of HGO1 membrane samples air aged for 5 years. (b) HGO1 film swelling in saturated d_6 -ethanol vapor after 2 and 4 years of air storage. Modeled Scattering Length Density (SLD) profiles calculated using NR scans of the HGO1 film (see the ESI file†). L corresponds to film thickness and the change in ρ is proportional to the amount of sorbed d_6 -ethanol.

The almost complete absence of swelling in ethanol, 1-propanol and 1-butanol revealed in our experiments with aged HGO membranes in combination with good swelling in water is rather surprising and is not a trivial result. Therefore, we studied swelling of freshly prepared GO membranes in a set of nine alcohols (methanol to 1-nonanol) and swelling of precursor HGO powder samples as a reference.

The swelling of three tested graphite oxide precursors (HGO1, HGO2, and HGO3; see the ESI file†) was found to be nearly identical (Fig. 2a). Fig. 2b shows that saturated swelling of the 1 week old HGO1 membrane is very similar to the swelling of precursor HGO powder in all alcohols. Remarkably the general trend found for swelling of Hummers graphite oxide at ambient temperature shows significant difference compared to that of Brodie graphite oxide, most remarkably for small alcohols (Fig. 3). Swelling of HGO in methanol, ethanol and 1-propanol is significantly stronger comparatively and corresponds to intercalation of at least 2–3 layers of solvent molecules. Note that the swelling of Hummers graphite oxide determined using $d(001)$ should not be directly interpreted



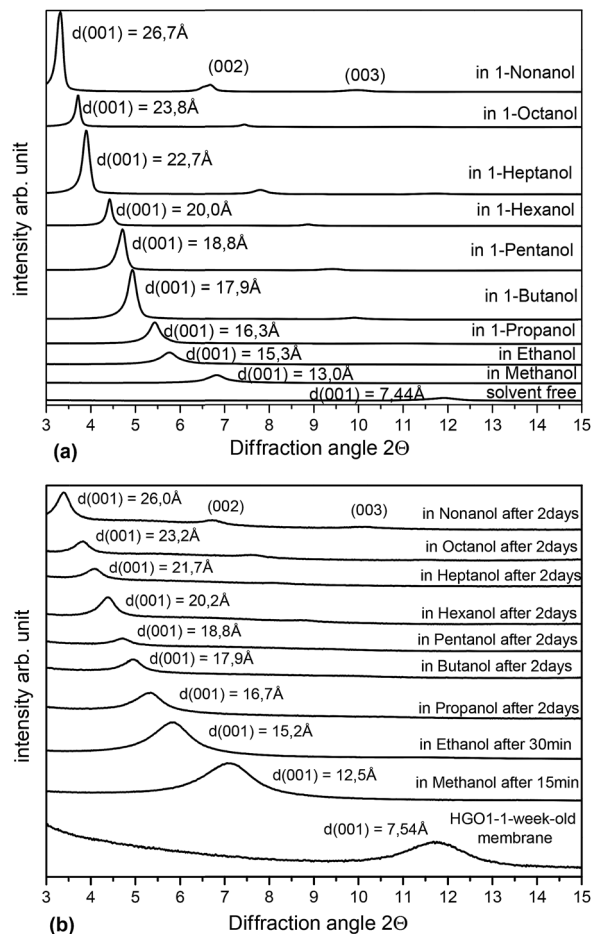


Fig. 2 XRD patterns recorded for HGO1 samples immersed in excess liquid alcohols: (a) powder (b) freshly prepared membrane (1 week) (Cu $K\alpha$ radiation).

using the number of intercalated layers. The position of the (001) reflection of Hummers graphite oxide is known to increase upon cooling due to effects of intrastatification and

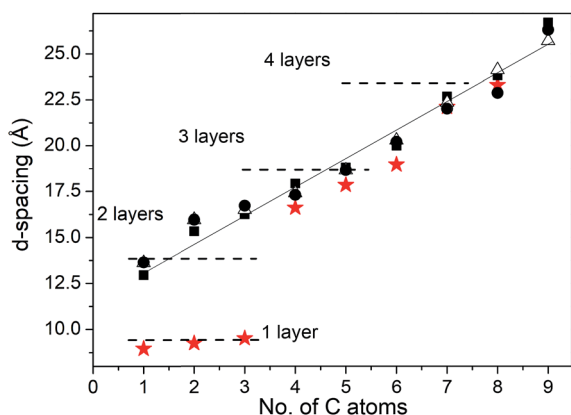


Fig. 3 Interlayer distance provided by $d(001)$ of HGO1 (■), HGO2 (●), and HGO3 (▲) powder samples and BGO powder (★) (ref. 30) in liquid alcohols with the number of carbon atoms $C = 1-9$ (methanol to 1-nonanol). Dashed lines show approximate swelling levels corresponding to the layer by layer intercalation of alcohols.

intrastatification.³² This is in strong contrast to Brodie graphite oxide which shows sharp transitions between *e.g.* 1-layer and 2-layer methanol solvate structures upon change of temperature and pressure.^{31,36}

Our experiments demonstrate that small alcohol molecules like methanol and ethanol diffuse into the HGO membrane structure rapidly. However, in contrast to the rather rapid swelling of powders (saturation achieved within a few minutes after immersion) rather slow kinetics of swelling was observed for HGO membranes in large alcohols (6 carbon atoms and higher). Moreover, the HGO2 and HGO3 membranes showed no swelling in the largest of alcohols (1-nonanol and 1-octanol) (see the ESI file†). The formation of the solvate phase in larger alcohols is observed first at near surface layers of the GO structure while the inner part remains unaffected for a certain period of time.

For example, experiments with freshly prepared HGO1 membranes immersed in 1-heptanol showed (001) reflections of both swollen and pristine phases. The position of the (001) reflection from the solvated phase did not shift significantly with time (21.5 Å to 22.1 Å in 12 hours) but the relative intensity increased over a period of hours reflecting penetration of the solvent into the subsurface parts of the multilayered structure (details in the ESI file†).

The difference in swelling between HGO membranes and powders becomes stronger for membranes stored over longer periods of time (0.6–2.5 years). The ageing of HGO1 membranes for 1–2.5 years results in two non-trivial effects. The first is the absence of swelling in 1-hexanol, 1-heptanol, 1-octanol and 1-nonanol (Fig. 4a). The second effect is the smaller swelling in ethanol providing $d(001) = 10.4$ Å which is ~ 5 Å smaller compared to that of freshly prepared HGO1 membranes. Remarkably, the swelling in 1-propanol, 1-butanol and 1-pentanol was almost unaffected by the ageing for 2.5 years. Similar data were also recorded using the HGO2 membrane sample studied for swelling in alcohols after storage for 1.5 years (see the ESI file†). Nonhomogeneous swelling of HGO membrane interlayers was detected using 2D XRD images which reveal significant diffuse scattering. The 2D image shown in Fig. 4a shows two pairs of spots from (001) reflections of the pristine and solvated phase and diffuse scattering and rings from the liquid solvent. The straight line of diffuse intensity provides evidence of the presence of continuous distribution of interlayer distances.

The mechanism behind the non-trivial changes in swelling properties of HGO membranes was investigated using characterization of freshly prepared and aged samples. XPS spectra recorded from the same piece of membrane as in ref. 16 after five years of storage showed significant ageing effects (Fig. 5a).

The relative intensity of three main peaks in the C 1s XPS spectra changed dramatically while the C/O ratio increased from 2.49 to 3.03. Chemical transformation of the HGO material over a long period of time *e.g.* due to the metastability effect reported in ref. 43 could be suggested to explain the evolution of the spectra.⁴³ However, the XPS data provide information for only about 1–2 surface layers of the multilayered membrane and could be strongly affected by surface related sorption of various molecules from the air. Surface contamination, *e.g.* sorption of



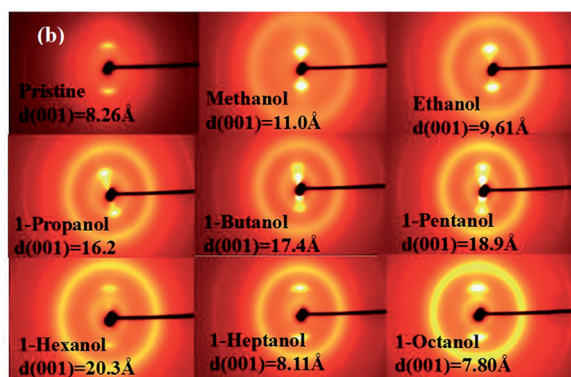
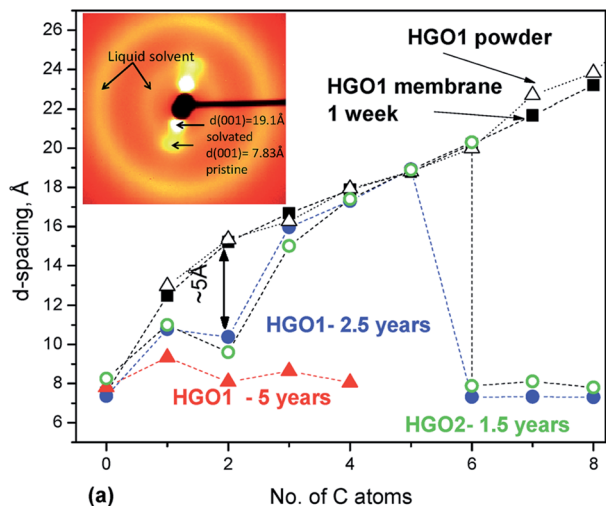


Fig. 4 (a) Interlayer distance ($d(001)$) for HGO1 powder (Δ) and membranes immersed in liquid alcohols: freshly prepared (1 week) sample (\blacksquare), sample stored in air for 2.5 years (\bullet), and sample stored in air for 5 years (\blacktriangle). The inset shows the 2D XRD image ($\lambda = 0.30996 \text{ \AA}$) recorded of the HGO2 membrane in 1-pentanol after 7.5 hours of immersion. (b) XRD images ($\lambda = 0.30996 \text{ \AA}$) recorded of the HGO2 membrane after 23–24 hours of immersion in liquid alcohols (see integrated scans and data for other samples in the ESI file†).

hydrocarbons, would contribute to the increased intensity of the C–C peak (285.0 eV). However, surface sorption would affect both graphite oxide powder and GO membranes very similarly.

Surprisingly, the changes in XPS spectra of precursor graphite oxide after 4 years of air storage appeared to be rather minor compared to the changes observed in spectra recorded from the aged membranes (Fig. 5b).

The effect of surface modification is also obvious in the XPS spectra recorded of membranes aged for several months (Fig. 5c). The relative intensity of peaks typically assigned to C–C and C–O (284.5 eV and 286.5 eV respectively) gradually changed following air storage. However, the changes in XPS spectra observed after 6 months of air storage were found to affect only surface layers of the membrane. XPS spectra recorded from the inner part of the same membrane showed the relative intensity of main peaks typical for freshly prepared samples (Fig. 5c). Therefore, the change of surface properties due sorption of some molecules from air also cannot be ruled out.

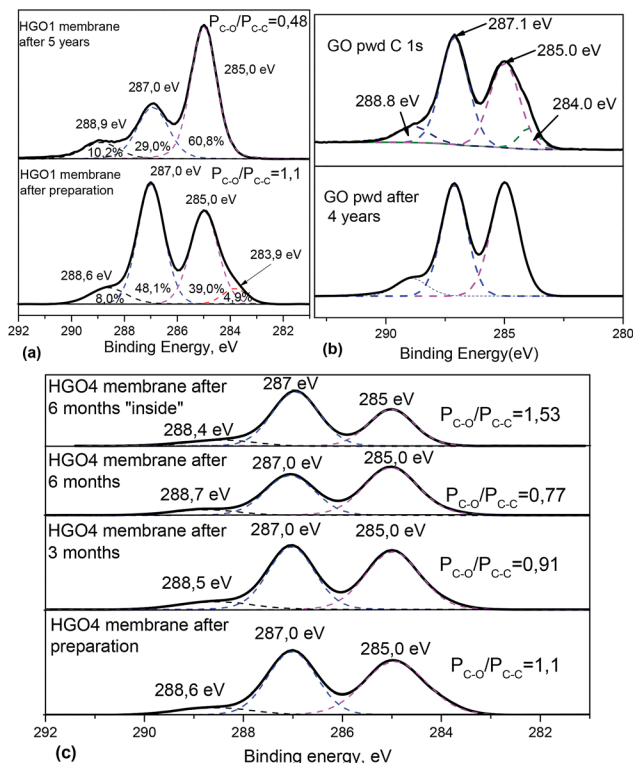


Fig. 5 (a) C 1s part of XPS spectra of the HGO1 membrane measured in 2013 (ref. 16) and after 5 years of ageing under ambient conditions. (b) FTIR spectra recorded from HGO1 membranes freshly prepared and aged for 2 years and 5 years. (c) C 1s XPS spectra of HGO membranes measured 1 week, 3 months, and 6 months after preparation on the surface and after mechanical removal of surface layers ("inside").

The FTIR spectra of aged samples showed different relative intensities of some main peaks, most notably a decrease in the intensity ratio for peaks due to C–C and C=O vibrations (Fig. 6).

Double bonded oxygen functional groups (carbonyls and carboxyls) can be found on the edges of GO flakes or on the edges of holes or vacancies on their planar part. A strong

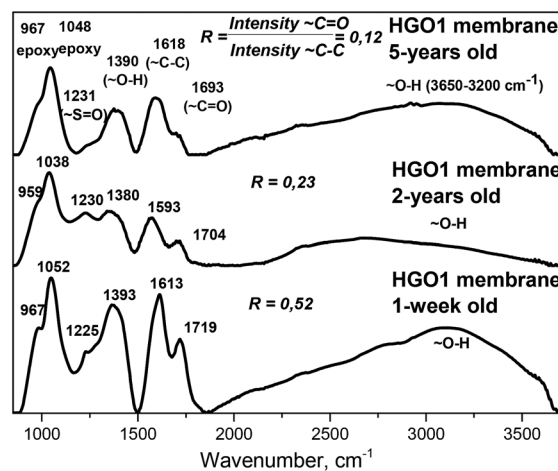


Fig. 6 XPS spectra recorded from the HGO1 powder sample shortly after synthesis (C/O = 2.47) and 4 years later after air storage (C/O = 2.38).



decrease in the intensity of the C=O peak in FTIR spectra indicates that some chemical modification of the GO flake edges occurs as a result of ageing and it is not related only to the surface part of the membrane sample.

Since the swelling of precursor graphite oxides remains nearly unchanged even after many years of air storage, we suggest that the ageing of membranes is likely to occur due to interactions between GO flakes in the multilayered structure rather than due to intrinsic metastability of GO. The difference between swelling of powders and membranes is evident already for freshly prepared samples. Graphite oxides are synthesized starting from graphite powder and preserve the original shape and size of graphite grains.²⁸ The entrance points of all interlayers are open for interaction with the bulk liquid surrounding the grains of graphite oxide. In contrast, GO membranes are formed by random re-stacking of individual sheets with nearly complete overlapping of all edges. The solvent must diffuse along a zigzag pathway starting from the surface of the membrane and around the overlapped edges of flakes to penetrate into sub-surface layers (Fig. 7).

The results presented above suggest the following two-step mechanism of membrane swelling:

- swelling of interlayers directly exposed to the bulk solvent occurs rapidly achieving saturation of the interlayer distance at least within minutes. Graphite oxide powder swells in one step.
- penetration of the solvent into subsurface layers occurs across/around overlapped flake edges. The overlaps (“junctions”) provide major limitations for diffusion of solvent into the bulk body of membranes. The overlaps also provide size limitation for penetration of larger molecules.

The GO flake edge overlap regions (interlayer “junctions”) are likely to become less flexible in the membranes stored for prolonged periods of time. The swelling of HGO membranes in the largest alcohols ceases over time as a result of the decreased ability of these interlayer junctions to expand.

The XPS and FTIR data (Fig. 5 and 6) demonstrate that the ageing of GO membranes starts from the surface and extends into the deeper sub-surface part of the membrane with time. Therefore, ageing can be connected to interaction of GO with air mediated by sorption of water (10–50 wt%, proportional to humidity^{24,28}).

A number of possible air contaminants might dissolve in water. These molecules will diffuse into the membrane

interlayers and stack/react at the junction points between overlapped edges of GO flakes.

The chemical interaction of GO edge functional groups (*e.g.* carboxyls) with neighboring GO flakes is more likely to occur at the regions of edge overlaps. If the number of connection points at the junction regions is small the GO lattice is still capable of swelling to almost full scale. When more connection points are added along the edges the openings available for diffusion of molecules become smaller. In the end only the smallest molecules (water) penetrate around the edge regions (Fig. 8).

It is unclear at the moment why the membranes aged for 0.6–2.5 years show significant decrease of swelling in ethanol (from ~15 Å in fresh to ~9.5–10.5 Å in aged samples) while the swelling in larger 1-propanol, 1-butanol and 1-pentanol remains unchanged. In fact, the decrease of $d(001)$ of HGO in ethanol to below ~15 Å is a rather straightforward indication of the bulk membrane ageing. For example, the samples used in our earlier study of HGO membrane swelling in water/ethanol mixtures were clearly affected by ageing since the $d(001)$ found in pure ethanol was found to be ~10.7 Å for two different membranes.¹⁶ Testing various membrane samples for swelling in ethanol revealed that in some cases ageing can be detected already after 6 months of air storage; in other samples swelling remained unchanged for longer periods of time up to 1 year.

The rate of GO membrane ageing is likely to depend on many parameters of sample storage, *e.g.* humidity levels, variations of humidity, temperature, *etc.* It cannot be ruled out that similar ageing occurs much faster (weeks) under different sample storage conditions, *e.g.* at very low or very high humidity or in colder/warmer climates. The difference of swelling between graphite oxide powder and HGO membranes was also found to be stronger for samples with larger average flake sizes (0.12 μm for HGO1 *vs.* 0.28 μm and 0.33 μm for HGO2 and HGO3 samples, respectively, see the ESI file†). Note that flake sizes of 0.1–0.3 μm are most common in GO membrane research due to the break up of larger flakes in the process of dispersion preparation by sonication. These types of membranes were recently named “conventional” to distinguish them from membranes composed of larger flakes.⁴⁵

The results presented in this study demonstrate that ageing must be considered as one of the key parameters which affect swelling and, as a result, permeation properties of HGO membranes. It is known that permeation rates reported for GO membranes in various studies are different by two orders of magnitude.³⁹ Therefore, ageing needs to be added to the list of

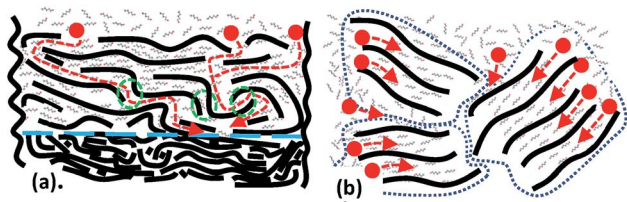


Fig. 7 Schematic representation of the difference in packing of GO flakes in HGO membranes and precursor powder. (a) Zigzag pathway of solvent molecules is typical for the membranes whereas the rate of diffusion is limited by the “junction” fronts along the overlapped flake edges (green ovals). (b). The graphite oxide structure provides entrance points, “gates” (●), to most of the inter-layers directly accessible from the bulk liquid solvent.

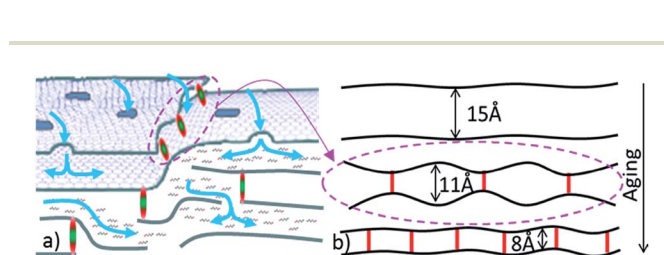


Fig. 8 (a) Schematic representation of the solvent permeation path across GO membrane multilayers with obstacles formed as a result of ageing along the edges of GO flakes. (b) Schematic illustration of how interconnections of GO flake edges could decrease maximal interlayer distance under swelling conditions.



parameters which affect GO membrane performance and require standardization.⁴⁰

Most of the studies related to properties of GO membranes do not report the exact time and conditions for their storage after preparation.

Conclusions

In summary, both precursor graphite oxides and freshly prepared HGO1 membranes are found to swell in the set of liquid alcohols (from methanol to 1-nonanol). The increase of interlayer spacing is found to be proportional to the size of alcohol molecules suggesting multilayered intercalation (up to ~26 Å in 1-nonanol).

Pronounced ageing effects were found for membranes stored in air. Ageing starts on the surface of the multilayered structure and slowly penetrates into the deeper regions. The lattice expansion due to swelling of HGO in ethanol and methanol becomes significantly smaller with time and disappears for 1-hexanol and larger alcohol molecules even after 0.6–2 years of ageing. The samples stored under ambient conditions for 5 years showed a nearly complete absence of swelling in alcohols but preserved significant swelling in water. The ageing of HGO membranes can be considered as a method to tune the swelling properties of HGO membranes for better selectivity in sorption of solvents and selective permeability.

The ageing of HGO membranes must be considered as one of the major parameters which affect their permeation properties. The rate of ageing is likely to be affected by the properties of membranes *vs.* conditions of sample storage and standardization is required in order to achieve better reproducibility of experimental results related to GO membrane applications.

Experimental section

The powder samples of commercial ACS Material graphite oxide (HGO1) and several batches of graphite oxides synthesized in our laboratory (HGO2, HGO3, and HGO4) were used to prepare membranes by vacuum filtration of aqueous dispersions. Characterization of precursor graphite oxides is available in the ESI file† (XPS, XRD, and FTIR). The degree of oxidation was found to be very similar with C/O in the range 2.30–2.47. Some HGO1 powder purchased in 2013 was re-evaluated in 2018 for ageing effects. Details of the membrane preparation procedure were the same as those in our previously published studies¹⁷ (see the ESI file† for details). Several membrane samples prepared using HGO were re-characterized after 1–5 years of air storage. The thickness of the membranes varied in the range 5–50 μm. More specifically, the data shown in Fig. 3 were collected using a 5 μm thick membrane. Thickness of the membranes shown in Fig. 4: 5 μm for 1 week old HGO1, 6 μm for 2.5 year old HGO1, 18 μm for HGO2 and 34 μm for the 5 year old sample. The membrane samples were stored at ambient humidity in the lab or an office environment with a typical humidity of 15–40% and temperature of 20–25 °C.

A HGO1 dispersion was used to prepare dispersions spin coated on Si blocks and studied using NR for ethanol and water

sorption.¹⁵ The sample of the HGO1 thin film on Si was characterized 3 times over 4 years for sorption of d₆-ethanol from saturated vapour. Neutron reflectivity experiments were performed in a specially designed humidity cell at the reflectometer SuperADAM at the Institute Laue-Langevin (ILL), Grenoble, France using a monochromatic beam with wavelength $\lambda = 5.19$ Å; details are available in the ESI† and elsewhere.²⁷ XRD characterization of graphite oxides and HGO membranes immersed in excess liquid solvents was performed using an in-house PANalytical X'pert diffractometer with Cu K α radiation in reflection mode and synchrotron radiation at beamline ID 11 ESRF, Grenoble, France with $\lambda = 0.30996$ Å. Several scans were typically recorded for solvent immersed samples until saturated swelling is achieved (5 min–2 days). Chemical composition of membranes was tested by XPS and FTIR spectroscopy, and AFM was used to evaluate flake size distribution; see details in the ESI.†

Conflicts of interest

There are no conflicts to declare.

Acknowledgements

The authors acknowledge funding from the European Union's Horizon 2020 Research and Innovation Program under grant agreement No. 785219 and the Swedish Research Council (Grant No. 2017-04173). A. R. and M. K. acknowledge support of the RFBR (Grant No. 18-33-00439). A. I. and A. T. acknowledge support from Kempestiftelserna. A. T. acknowledges the COST Action CA 15107 "Multi-Functional Nano-Carbon Composite Materials Network (MultiComp)". We also acknowledge support of the Vibrational Spectroscopy Platform of Umeå, University and A. Shchukarev for technical support with XPS. We acknowledge support from the ESRF for experiments performed at ID11 and technical assistance of Carlotta Giacobbe. We thank the ILL staff for technical support.

Notes and references

- 1 D. A. Dikin, S. Stankovich, E. J. Zimney, R. D. Piner, G. H. B. Dommett, G. Evmenenko, S. T. Nguyen and R. S. Ruoff, *Nature*, 2007, **448**, 457–460.
- 2 W. L. Xu, C. Fang, F. Zhou, Z. Song, Q. Liu, R. Qiao and M. Yu, *Nano Lett.*, 2017, **17**, 2928–2933.
- 3 Z. T. Luo, Y. Lu, L. A. Somers and A. T. C. Johnson, *J. Am. Chem. Soc.*, 2009, **131**, 898–899.
- 4 M. Krueger, S. Berg, D. Stone, E. Strelcov, D. A. Dikin, J. Kim, L. J. Cote, J. X. Huang and A. Kolmakov, *ACS Nano*, 2011, **5**, 10047–10054.
- 5 R. R. Nair, H. A. Wu, P. N. Jayaram, I. V. Grigorieva and A. K. Geim, *Science*, 2012, **335**, 442–444.
- 6 H. Li, Z. Song, X. Zhang, Y. Huang, S. Li, Y. Mao, H. J. Ploehn, Y. Bao and M. Yu, *Science*, 2013, **342**, 95–98.
- 7 H. P. Boehm, A. Clauss and U. Hofmann, *J. Chim. Phys. Phys.-Chim. Biol.*, 1961, **58**, 141–147.



- 8 P. Z. Sun, F. Zheng, M. Zhu, Z. G. Song, K. L. Wang, M. L. Zhong, D. H. Wu, R. B. Little, Z. P. Xu and H. W. Zhu, *ACS Nano*, 2014, **8**, 850–859.
- 9 Y. Han, Z. Xu and C. Gao, *Adv. Funct. Mater.*, 2013, **23**, 3693–3700.
- 10 R. Liu, G. Arabale, J. Kim, K. Sun, Y. Lee, C. Ryu and C. Lee, *Carbon*, 2014, **77**, 933–938.
- 11 Y. P. Tang, D. R. Paul and T. S. Chung, *J. Membr. Sci.*, 2014, **458**, 199–208.
- 12 R. S. Steinberg, M. Cruz, N. G. A. Mahfouz, Y. Qiu and R. H. Hurt, *ACS Nano*, 2017, **11**, 5670–5679.
- 13 E. S. Bober, L. C. Flowers, P. K. Lee, D. E. Sestrich, C.-M. Wong, W. Gillam Sherman, S. Johnson and R. H. Horowitz, *Research and Development Progress Report No. 544*, US Department of the Interior, reprints from the collection of the University of Michigan Library, 1970, pp. 1–113.
- 14 T. Szabo, O. Berkesi, P. Forgo, K. Josepovits, Y. Sanakis, D. Petridis and I. Dekany, *Chem. Mater.*, 2006, **18**, 2740–2749.
- 15 A. Vorobiev, A. Dennison, D. Chernyshov, V. Skrypnichuk, D. Barbero and A. V. Talyzin, *Nanoscale*, 2014, **6**, 12151–12156.
- 16 A. V. Talyzin, T. Hausmaninger, S. J. You and T. Szabo, *Nanoscale*, 2014, **6**, 272–281.
- 17 A. Klechikov, J. C. Yu, D. Thomas, T. Sharifi and A. V. Talyzin, *Nanoscale*, 2015, **7**, 15374–15384.
- 18 J. C. Derksen and J. R. Katz, *Recl. Trav. Chim. Pays-Bas*, 1934, **53**, 652–669.
- 19 J. C. Ruiz and D. M. C. Macewan, *Nature*, 1955, **176**, 1222–1223.
- 20 A. Lerf, A. Buchsteiner, J. Pieper, S. Schottl, I. Dekany, T. Szabo and H. P. Boehm, *J. Phys. Chem. Solids*, 2006, **67**, 1106–1110.
- 21 A. V. Talyzin, V. L. Solozhenko, O. O. Kurakevych, T. Szabo, I. Dekany, A. Kurnosov and V. Dmitriev, *Angew. Chem., Int. Ed.*, 2008, **47**, 8268–8271.
- 22 A. Klechikov, S. You, L. Lackner, J. Sun, A. Iakunkov, A. Rebrikova, M. Korobov, I. Baburin, G. Seifert and A. V. Talyzin, *Carbon*, 2018, **140**, 157–163.
- 23 T. Daio, T. Bayer, T. Ikuta, T. Nishiyama, K. Takahashi, Y. Takata, K. Sasaki and S. M. Lyth, *Sci. Rep.*, 2015, **5**, 11807.
- 24 M. V. Korobov, A. V. Talyzin, A. T. Rebrikova, E. A. Shilayeva, N. V. Avramenko, A. N. Gagarin and N. B. Ferapontov, *Carbon*, 2016, **102**, 297–303.
- 25 Y. H. Cho, H. W. Kim, H. D. Lee, J. E. Shin, B. M. Yoo and H. B. Park, *J. Membr. Sci.*, 2017, **544**, 425–435.
- 26 F. Barroso-Bujans, S. Cerveny, A. Alegria and J. Colmenero, *Carbon*, 2010, **48**, 3277–3286.
- 27 A. Klechikov, J. H. Sun, A. Vorobiev and A. V. Talyzin, *J. Phys. Chem. C*, 2018, **122**, 13106–13116.
- 28 U. Hofmann, A. Frenzel and E. Csalán, *Justus Liebigs Ann. Chem.*, 1934, **510**, 1–41.
- 29 A. R. Garcia, J. Canoruiz and D. M. C. Macewan, *Nature*, 1964, **203**, 1063–1064.
- 30 A. Klechikov, J. H. Sun, I. A. Baburin, G. Seifert, A. T. Rebrikova, N. V. Avramenko, M. V. Korobov and A. V. Talyzin, *Nanoscale*, 2017, **9**, 6929–6936.
- 31 A. V. Talyzin, B. Sundqvist, T. Szabo, I. Dekany and V. Dmitriev, *J. Am. Chem. Soc.*, 2009, **131**, 18445–18449.
- 32 S. J. You, B. Sundqvist and A. V. Talyzin, *ACS Nano*, 2013, **7**, 1395–1399.
- 33 A. B. Bourlinos, D. Gournis, D. Petridis, T. Szabo, A. Szeri and I. Dekany, *Langmuir*, 2003, **19**, 6050–6055.
- 34 F. A. Delacruz and D. M. C. Macewan, *Kolloid Z. Z. Polym.*, 1965, **203**, 36–41.
- 35 M. Herrera-Alonso, A. A. Abdala, M. J. McAllister, I. A. Aksay and R. K. Prud'homme, *Langmuir*, 2007, **23**, 10644–10649.
- 36 S. J. You, S. Luzan, J. C. Yu, B. Sundqvist and A. V. Talyzin, *J. Phys. Chem. Lett.*, 2012, **3**, 812–817.
- 37 L. Huang, Y. R. Li, Q. Q. Zhou, W. J. Yuan and G. Q. Shi, *Adv. Mater.*, 2015, **27**, 3797–3802.
- 38 S. J. Kim, D. W. Kim, K. M. Cho, K. M. Kang, J. Choi, D. Kim and H. T. Jung, *Sci. Rep.*, 2018, **8**, 1959.
- 39 C. A. Amadei and C. D. Vecitis, *J. Phys. Chem. Lett.*, 2016, **7**, 3791–3797.
- 40 C. A. Amadei, P. Arribas and C. D. Vecitis, *Carbon*, 2018, **133**, 398–409.
- 41 C. N. Yeh, K. Raidongia, J. J. Shao, Q. H. Yang and J. X. Huang, *Nat. Chem.*, 2015, **7**, 166–170.
- 42 D. N. Voylov, I. N. Ivanov, V. I. Bykov, S. B. Tsybenova, I. A. Merkulov, S. A. Kurochkin, A. P. Holt, A. M. Kisliuk and A. P. Sokolov, *RSC Adv.*, 2016, **6**, 78194–78201.
- 43 S. Kim, S. Zhou, Y. K. Hu, M. Acik, Y. J. Chabal, C. Berger, W. de Heer, A. Bongiorno and E. Riedo, *Nat. Mater.*, 2012, **11**, 544–549.
- 44 A. V. Talyzin, G. Mercier, A. Klechikov, M. Hedenstrom, D. Johnels, D. Wei, D. Cotton, A. Opitz and E. Moons, *Carbon*, 2017, **115**, 430–440.
- 45 Q. Yang, Y. Su, C. Chi, C. T. Cherian, K. Huang, V. G. Kravets, F. C. Wang, J. C. Zhang, A. Pratt, A. N. Grigorenko, F. Guinea, A. K. Geim and R. R. Nair, *Nat. Mater.*, 2017, **16**, 1198–1203.

